

# Bioavailability of Iron Sensed by a Phytoplanktonic Fe-Bioreporter

CHRISTEL S. HASSLER AND  
MICHAEL R. TWISS\*

Department of Biology and Center for the Environment,  
Clarkson University, Potsdam, New York 13699-5805

This study describes a short-term (12 h) evaluation of iron (Fe) bioavailability to an Fe-dependent cyanobacterial bioreporter derived from *Synechococcus* PCC 7942. Several synthetic ligands with variable conditional stability constants for Fe(III) ( $K^*$  of  $10^{19.8}$  to  $10^{30.9}$ ), in addition to several defined natural Fe-binding ligands and a fulvic acid of aquatic origin (Suwannee River), were used to elucidate the forms of Fe that are discerned by this phytoplanktonic microbe: Fe-HEBD (log conditional stability constant,  $K^*$ , = 28.1, HEBD = *N,N'*-di(2-hydroxybenzyl)ethylenediamine-*N,N'*-diacetic acid monohydrochloride hydrate), Fe-HDFB ( $K^*$  = 30.9, DFB = desferroxamine B), Fe-ferrichrome ( $K^*$  = 23.2), Fe-DTPA ( $K^*$  = 21.1, DTPA = diethylenetri-nitripentaacetic acid), Fe-(8HQS)<sub>2</sub> ( $K^*$  = 20.4, 8HQS = 8-hydroxyquinoline-5-sulfonic acid), Fe-CDTA ( $K^*$  = 19.8, CDTA = *trans*-1,2-cyclohexylenedinitrilotetraacetic acid), and Fe-EDTA ( $K^*$  = 19.2). Iron bioavailability sensed by the bioreporter was related to diffusion limitation and activity of high-affinity transporters rather than by siderophore secretion. Iron complexed with a  $K^*$  < 23.2 contributes to the bioavailable pool; bioavailability could be explained by disjunctive ligand exchange considerations and fully, partially, and nonbioavailable complexes could be distinguished according to their conditional stability constant. The use of Fe-bioreporters provides a relevant measurement of bioavailability to an important group of primary producers in freshwaters (cyanobacteria) and is thus a promising technique for understanding Fe cycling in aquatic systems.

## Introduction

Iron (Fe) is an essential nutrient known to limit primary productivity in vast regions of the oceans (e.g., (1)), and in some large lakes (e.g., (2, 3)). Given the important nutritive role played by Fe in phytoplankton metabolism and their respective roles in the global carbon cycle, much interest has been focused on understanding Fe uptake and limitation to phytoplankton (e.g., (4)). In situations of steady state between the surface of the organism and the solution, the Hudson and Morel  $Fe'$  model describes the direct uptake of Fe(III) in its free ion and soluble  $Fe(OH)_x$  forms (defined as  $Fe'$ ) by eukaryotic phytoplankton (see ref 5). Iron bioavailability to phytoplankton is a challenge due to the low solubility of Fe(III), an active redox cycle, slow reaction kinetics, important associations of Fe(III) with poorly defined organic ligands that can be photodegraded under natural conditions, and highly specific biological uptake strategies. Both the

diffusion and the kinetic nature of chemical reactions have been examined for Fe using growth responses and metal internalization by coastal and oceanic phytoplankton (5, 6). As an illustration of the complexity of iron bioavailability, FeEDTA was not bioavailable to several oceanic phytoplankton (e.g., (5, 7, 8)), whereas weaker and stronger iron complexes were bioavailable to prokaryotic and eukaryotic phytoplankton (9–11). The recent development of an Fe-dependent bioreporter (12) presents the unique advantage of providing a sensitive and rapid (12 h) measurement of Fe bioavailability at the spatial and temporal scale of living microorganisms. In general, the capacity of an organism to out compete chelators for Fe in solution will depend on its biological requirement, mode of iron acquisition (reductase (8), siderophore (13), physiological status (e.g., induction of high-affinity Fe transporters (6), or siderophore excretion (13)), and ability to recognize Fe-siderophore complexes (9, 10). In both eukaryotic and prokaryotic phytoplankton, exogenous Fe must first interact with a siderophore, a reductase, or a transporter prior to being internalized by the organism. In the case of enhanced Fe bioavailability (i.e., higher than predicted by  $[Fe']$ ), complexed Fe might contribute to the bioavailable pool of Fe. Under these circumstances, Fe must be exchanged from a ligand in solution (L) to a biological binding site (X) either in solution (e.g., siderophore) or at the surface of the organism (e.g., reductase or transporter). Adjunctive or disjunctive exchange can be considered to control iron bioavailability (cf., (14)). Due to low free Fe concentrations and high stability constants, adjunctive exchange mechanisms with the formation of ternary complexes (L-Fe-X) might be favored. Since the formation of intermediate ternary complexes is poorly characterized, disjunctive exchange will be considered in this study. The formation of Fe-X and Fe-L is usually limited by the water-loss rate ( $k_{-w}$ , Eigen-Wilkins mechanisms, see refs 15, 16), which is poorly dependent upon the nature of the ligand. As a consequence, the dissociation constant of a Fe complex is inversely related to the conditional stability constant of the Fe complex, and thus, exchange of Fe can be predicted on the basis of the stability constants and concentrations of Fe-L and Fe-X.

In the present study, a cyanobacterial Fe-dependent bioreporter (KAS 100) developed to assess Fe limitation under natural conditions (17) was used to understand the Fe-uptake process and Fe bioavailability. Production of bioluminescence by the bioreporter occurs under iron deficiency, when no more intracellular Fe is available to bind the repressor (Fur), leading to its release from DNA and expression of the targeted gene [*isiAB*; (17, 18)]. Both dose-response and Fe-55 bioaccumulation experiments (12 h and 40 min) were used to understand the effect of Fe chemical speciation on the bioavailability of complexed Fe. Several synthetic ligands with variable conditional stability constants for Fe(III), in addition to several defined natural Fe-binding ligands and a fulvic acid of aquatic origin, are used to elucidate the forms of Fe that are discerned by this cyanobacterium.

## Materials and Methods

**Growth Media and Strain Preparation.** Particulars of the protocol for maintaining the *Synechococcus* bioreporter are detailed in ref 17; the experimental conditions used here provide a maximal bioluminescent response by the cyanobacterial bioreporter (17). In brief, the Fe-bioreporter was maintained in a defined medium (BG11 (19)) wherein iron ammonium citrate was replaced by equimolar amounts of

\* Corresponding author phone: (315)268-2359; fax: (315)268-7118; e-mail: mtwiss@clarkson.edu.

FeCl<sub>3</sub>, resulting in an enriched Fe' concentration of 33 μM ([Fe]<sub>tot</sub> = 37 μM). Iron speciation was calculated using MINEQL+ (ver. 4.5). Cultures were maintained at room temperature (20–25 °C) under constant light (18–20 μmol quanta·m<sup>-2</sup>·s<sup>-1</sup>) and were transferred monthly into fresh media (20-fold dilution).

Prior to experimental use, the bioreporter was acclimated to mild Fe deficiency in a two-step transfer into new media. *Synechococcus* was maintained in Fe-enriched BG11 (5–8 weeks) then transferred (20-fold dilution) into a medium (medium 1, see below) resulting in a 2-fold lower [Fe'] ([Fe'] = 14 μM). Medium 1 consisted of a 1:1 mix of non-Fe-enriched BG11 (Sigma)/Fraquil Fe-enriched ((20), [Fe]<sub>tot</sub> = 1 μM instead of 0.45 μM). After 3–4 days of exponential growth, *Synechococcus* was transferred (20-fold dilution) into Fraquil (medium 2) resulting in [Fe'] of 0.68 pM. The bioreporter was used following 2–4 days of exponential growth in medium 2. The bioreporter was maintained in an incubation chamber (Percival Scientific) at 18–19 °C under constant light (fluorescent tubes, 50–55 μmol quanta·m<sup>-2</sup>·s<sup>-1</sup>) and gyrotary shaking (100 rpm) during acclimation.

Biological and chemical contamination was avoided by manipulation under a HEPA laminar flow hood, sterilization of solutions by 0.2-μm filtration (acid-washed polycarbonate membrane filters) or microwave, use of deionized water (MilliPore Gradient), and the use of acid-washed polycarbonate containers (soaked in 0.5% HCl [Fisher, trace metal grade], rinsed 7-fold with deionized water, and dried under HEPA laminar flow). Stock solutions of macronutrients were treated with Chelex-100 resin (BioRad, (21)) to reduce trace metal contamination. *Synechococcus* was grown in the presence of 20 mg·L<sup>-1</sup> of kanamycin and spectinomycin to ensure the genetic integrity of the bioreporter, but the antibiotics were omitted from the experimental test media.

**Experimental Solutions.** The effect of Fe speciation on the bioreporter was assessed using two types of solutions (pH 6.8–6.9) based on Fraquil medium (NaNO<sub>3</sub>, 10<sup>-4</sup> M; K<sub>2</sub>-HPO<sub>4</sub>, 10<sup>-5</sup> M; CaCl<sub>2</sub>, 2.5 × 10<sup>-4</sup> M; MgSO<sub>4</sub>, 1.5 × 10<sup>-4</sup>; NaHCO<sub>3</sub>, 1.5 × 10<sup>-4</sup> M): (i) Fraquil media with various Fe' concentrations (Table 1) and (ii) solutions with constant total Fe concentration (10<sup>-7</sup> M) and various concentrations of ligands (Table 2) in the absence of micronutrients. For the Fraquil media with various [Fe], Fe speciation was manipulated by addition of variable total concentrations of Fe and EDTA. Free concentrations of all other trace metals present in the Fraquil medium were kept constant. The effect of various amounts of ligands to decrease the bioavailability of Fe was assessed by using both synthetic (EDTA [Sigma], CDTA [Fluka], DTPA [Fluka], 8HQ5 [8-hydroxyquinoline-5-sulfonic acid, Sigma], HEBD [*N,N'*-di(2-hydroxybenzyl)ethylenediamine-*N,N'*-diacetic acid monohydrochloride hydrate, Sigma]), and natural organic ligands (Suwannee River fulvic acid [SRFA; International Humic Substance Society, St. Louis, MO], desferroxamine B [DFB, Sigma], and ferrichrome [Sigma]). DFB and ferrichrome are hydroxamate-type siderophores similar to siderophores excreted by *Synechococcus* PCC 7942 (22). Stock solutions of synthetic ligands were prepared at 10<sup>-3</sup> M and adjusted to pH 6 using trace metal grade NaOH (Alfa-Aesar) and HNO<sub>3</sub> (Seastar). Iron contamination was checked with graphite furnace atomic absorption spectroscopy (GFAAS, Perkin-Elmer AA600). To reduce photo- and thermal degradation, solutions were maintained in the dark at 4 °C or -18 °C. For each ligand (except SRFA), the conditional stability constant for the major Fe complex formed (see Table 2) was calculated using the stability constant obtained from NIST (2004, ver. 8) transformed to an ionic strength of zero using the Davies equation prior to insertion in the MINEQL+ (ver. 4.5) database.

**Bioreporter Assay.** Prior to experimentation, bioreporters were isolated by gentle filtration (<30 kPa) onto a 0.4-μm

**TABLE 1. Iron Speciation in Experimental Media Used for Calibration<sup>a</sup>**

[Fe] <sub>tot</sub> (M)	-log[Fe <sup>3+</sup> ]	[Fe'] (M)	[FeEDTA] (M)
4.5 × 10 <sup>-7</sup>	19.9	1.9 × 10 <sup>-11</sup>	3.9 × 10 <sup>-7</sup>
1.0 × 10 <sup>-7</sup>	20.5	4.3 × 10 <sup>-11</sup>	8.7 × 10 <sup>-8</sup>
4.5 × 10 <sup>-8</sup>	20.9	1.9 × 10 <sup>-12</sup>	3.9 × 10 <sup>-8</sup>
1.0 × 10 <sup>-8</sup>	21.5	4.3 × 10 <sup>-13</sup>	8.7 × 10 <sup>-9</sup>
7.5 × 10 <sup>-9</sup>	21.7	3.2 × 10 <sup>-13</sup>	6.6 × 10 <sup>-9</sup>
4.5 × 10 <sup>-9</sup>	21.9	1.9 × 10 <sup>-13</sup>	3.9 × 10 <sup>-9</sup>
1.0 × 10 <sup>-9</sup>	22.5	4.3 × 10 <sup>-14</sup>	8.7 × 10 <sup>-10</sup>
4.5 × 10 <sup>-10</sup>	22.9	1.9 × 10 <sup>-14</sup>	3.9 × 10 <sup>-10</sup>
2.8 × 10 <sup>-10</sup>	23.2	1.2 × 10 <sup>-14</sup>	2.4 × 10 <sup>-10</sup>
1.0 × 10 <sup>-8</sup>	22.5	4.3 × 10 <sup>-14</sup>	8.7 × 10 <sup>-9</sup>
4.5 × 10 <sup>-9</sup>	22.9	1.9 × 10 <sup>-14</sup>	3.9 × 10 <sup>-9</sup>
2.8 × 10 <sup>-9</sup>	23.2	1.2 × 10 <sup>-14</sup>	2.4 × 10 <sup>-9</sup>
5.5 × 10 <sup>-10</sup>	23.2	1.3 × 10 <sup>-14</sup>	4.8 × 10 <sup>-10</sup>
1.4 × 10 <sup>-9</sup>	23.2	1.3 × 10 <sup>-14</sup>	1.2 × 10 <sup>-9</sup>
5.5 × 10 <sup>-9</sup>	23.2	9.6 × 10 <sup>-15</sup>	4.8 × 10 <sup>-9</sup>
8.3 × 10 <sup>-9</sup>	23.2	7.5 × 10 <sup>-15</sup>	7.2 × 10 <sup>-9</sup>

<sup>a</sup> Total iron ([Fe]<sub>tot</sub>), free iron [Fe<sup>3+</sup>], weakly bound iron ([Fe'] = Σ[Fe<sup>3+</sup>] + major [Fe(OH)<sub>x</sub>] species in solution; for Fraquil [Fe(OH)<sub>3</sub>(aq)] and [Fe(OH)<sub>2</sub><sup>+</sup>] and [FeEDTA] are shown. Data from two sets of solutions (separated by an empty row) are presented: (1) the solution used for standard calibration and (2) solutions used to verify the contribution of complexed iron to the measured bioavailability. The first set of solutions was obtained by decreasing [Fe]<sub>tot</sub>, slightly increasing [Ca]<sub>tot</sub>, and keeping constant the concentrations of EDTA (5 × 10<sup>-6</sup> M) and the other trace metals present in the Fraquil medium (free metal concentrations, see Morel et al. (20)). In this case, [Fe<sup>3+</sup>] is proportional to all iron species in solutions. The second set of solutions was obtained by increasing 10-fold the concentration of every trace metal and EDTA as compared from Fraquil (upper part) or by varying EDTA, Fe, and other trace metals so that the proportionality observed in set 1 does not exist (lower part).

pore-size polycarbonate membrane filter, washed with a chelating solution (1 min in 10<sup>-5</sup> M EDTA in macronutrients from the Fraquil medium, except Ca and Mg), rinsed 3-fold in trace metal-free Fraquil medium, and resuspended in 1–2 mL of trace metal-free Fraquil medium. The bioreporter was added in the various experimental solutions to an initial concentration of 8–10 × 10<sup>4</sup> cell·mL<sup>-1</sup> (estimated surface area of 7.4–9.2 × 10<sup>5</sup> μm<sup>2</sup>·mL<sup>-1</sup> assuming spherical cells), as determined using an electronic particle counter (Coulter Counter, Multisizer 3). Following a 12 h incubation under constant light (50–70 μmol quanta·m<sup>-2</sup>·s<sup>-1</sup>) at 19 °C, cellular density and bioluminescence were measured for each experimental condition. Decanal (Sigma) was added (final concentration = 60 μM) to provide a substrate to react (5 min in the dark) with the bacterial luciferase. Bioluminescence was determined over 20 s using a luminometer (Zylyx FB 14; following a 15 s delay in the dark) and normalized to cell density. Each complete experiment was performed at least twice with 2–3 replicates per treatment.

**Iron Bioaccumulation Experiments.** Since the expression of bioluminescence shows a hyperbolic dependency upon photon flux intensity of photosynthetically active radiation during exposure, most experiments were performed under constant light (17). Short-term (40 min) Fe-uptake experiments, in light (65–70 μmol quanta·m<sup>-2</sup>·s<sup>-1</sup>) or in dark at 19 °C, were performed in Fraquil (where micronutrients were omitted) in the presence of 10<sup>-7</sup> M total Fe and various concentrations of EDTA, CDTA, and DFB. *Synechococcus* growing exponentially at two levels of exogenous Fe (medium 1 and medium 2) were used in these experiments. Long-term (12 h) exposures were performed under light (65–70 μmol quanta·m<sup>-2</sup>·s<sup>-1</sup>) at 19 °C with various [Fe'] in complete Fraquil media. Radioactive Fe (<sup>55</sup>Fe]-FeCl<sub>3</sub>, specific activity 69.64 mCi·mg<sup>-1</sup>, Perkin-Elmer Life Sciences) was used to measure Fe uptake by the bioreporter. <sup>55</sup>Fe was added at 0.025 versus 0.05 μCi·mL<sup>-1</sup> to biomass levels of 8 versus 20

**TABLE 2. Description of Ligands Used to Measure Fe Bioavailability<sup>a</sup>**

ligand (L)	major Fe complex at pH 6.9 (% total Fe)	K	K*
desferrioxamine B (DFB)	FeHL (100%)	42.7	30.9
<i>N,N'</i> -di[2-hydroxybenzyl]ethylenediamine- <i>N,N'</i> -diacetic acid monohydrochloride hydrate (HEBD)	FeL (100%)	41.6	28.1
ferrichrome	FeL (100%)	31.0	23.2
diethylenetrinitriolpentaacetic acid (DTPA)	FeL (99.8%)	31.2	21.1
8-hydroxyquinoline-5-sulfonic acid (8HQS)	FeL <sub>2</sub> (0.3%) <sup>c</sup>	23.4	20.4
trans-1,2-cyclohexylenedinitrilotetraacetic acid (CDTA)	FeL (99.7%)	32.7	19.8
ethylenedinitrilotetraacetic acid (EDTA)	FeL (84.9%)	27.7	19.2
Suwannee River fulvic acid (SRFA)	FeL <sub>a</sub> <sup>b</sup>	L <sub>a</sub> = 33	
	FeL <sub>b</sub> <sup>b</sup>	L <sub>b</sub> = 5	

<sup>a</sup> Ferrichrome and DFB are hydroxamate siderophores produced by fungi; HEBD, EDTA, CDTA, DTPA, and 8HQS are synthetic organic ligands, whereas SRFA is a natural organic ligand. The major complex present was calculated using MINEQL+ (ver. 4.5) and an updated database (NIST, 2004, ver. 8; stability constants were adjusted to 0 ionic strength using the Davies equation prior to being used in MINEQL). <sup>b</sup> Conditional stability constants were calculated by dividing the corresponding *K* by the ratio total ligand/free ligand in the absence of iron. Stability constants for SRFA were derived from VisualMINETQ (J. P. Gustafsson, KTH, Department of Land and Water Resources Engineering, Stockholm, SW; ver. 2.31) using all default parameters considering 100% of colored dissolved organic matter as fulvic acid. Since complexation of Fe by FA is complex and poorly characterized, no conditional stability constants were calculated. <sup>c</sup> On the basis of the stability constant from NIST, for 8-fold excess (8HQS)<sub>2</sub>, only 16.4% of Fe(8HQS)<sub>2</sub> can be calculated (competition with H<sup>+</sup>, *K*<sub>H8HQS</sub> = 8.78), although a maximal luminescence (i.e., decrease of iron bioavailability from 10<sup>-7</sup> to 10<sup>-9</sup> M) is measured. An increase of 10% of the log *K*<sub>Fe(8HQS)<sub>2</sub></sub> resulted in 26.6% and 97.1% Fe(8HQS)<sub>2</sub> for 1- and 8-fold excess (8HQS)<sub>2</sub>, respectively. Since the stability constants defined in NIST could not explain our observations, the relative bioavailability of 8HQS was calculated assuming a negligible competition for the binding to the proton.

× 10<sup>4</sup> cells·mL<sup>-1</sup>; short-term exposures required higher radioactivity and initial biomass. Initial dissolved Fe and <sup>55</sup>-Fe were determined by GFAAS and liquid scintillation (LKB Wallac RackBeta model 1219), respectively. At the end of the accumulation phase, *Synechococcus* was washed with a modified oxalate solution (0.1 M, pH 8) to determine intracellular Fe. The concentration of EDTA and citric acid recommended in the oxalate solution (23) was decreased 10-fold (to 5 mM) in order to avoid toxicological effects (24); in addition, NaCl and KCl were omitted to reduce ionic strength. The washing efficiency of the oxalate solution for various washing times (24) was optimal after 20 min. Surface-adsorbed Fe was determined by subtracting intracellular Fe from the total particulate Fe. To express internalization fluxes, cellular density was used to normalize intracellular Fe.

**Results**

**Calibration of the Bioreporter.** Cellular bioluminescence of the bioreporter is related in a sigmoidal dose–response manner to the free Fe concentration (pFe or –log [Fe<sup>3+</sup>]) in the Fraquil media (Figure 1A, circles). Cells in the experimental treatments were growing during the 12 h exposure period. Cellular bioluminescence increased at pFe ≥ 20.9, as expected if *PisIAB* was de-repressed (and thus Fe–Fur dissociates) by a decrease in the bioavailable level of Fe. Bioluminescence was related to pFe up to pFe 22.5 (linear slope close to 1 in a log–log graph (0.97), *r*<sup>2</sup> = 0.95, *n* = 8). For very low free Fe concentrations (pFe ≤ 22.9), the response of the bioreporter reached a plateau of maximal response (Fe–Fur fully dissociated). Thus, the bioreporter can be used to sense Fe bioavailability for low free Fe concentrations (pFe 20.9–22.5).

**Fe Bioavailability in the Chemically Defined Media.** If pFe is proportional to all Fe species in solution (i.e., [Fe]<sub>tot</sub> variable, constant [EDTA] = 5 μM, Figure 1A circles, Table 1) then it cannot be concluded that the bioreporter responded exclusively to [Fe<sup>3+</sup>] in media. For if we assume that the bioreporter responds exclusively to [Fe<sup>3+</sup>] (i.e., Fe<sup>3+</sup> is the only bioavailable form), then the cellular luminescence would be constant for the same pFe. As shown in Figure 1A (squares), the response of the bioreporter cannot be related only to pFe. Variable responses observed in Figure 1A can be reduced by plotting the cellular luminescence against total Fe concentrations ([Fe]<sub>tot</sub>) in solution (Figure 1B), demonstrating that other Fe species (in addition to Fe<sup>3+</sup>) could interact with

the Fe–Fur complex inside the organism and reduce bioluminescence. On the basis of MINEQL+ calculations, free Fe is a minor species present in solution (<0.001%), whereas other Fe species predominate (0.3% Fe(OH)<sub>x</sub>, 12.6% FeO–HEDTA, 87% FeEDTA). When the response of the bioreporter is presented as a function of the sum concentration of all Fe–EDTA complexes a sigmoidal relationship is evident (Figure 1C), suggesting that the Fe complexed by EDTA significantly contributes to bioluminescence—within the construct of this experiment we cannot discern which EDTA–Fe species directly contributes to Fe bioavailability. The bioavailability of Fe bound to EDTA indicates that weaker Fe complexes present in solution, such as Fe(OH)<sub>x</sub>, were also bioavailable to this bioreporter. In this case, response of the bioreporter must be related to [Fe]<sub>tot</sub> (i.e., [Fe] that is bioavailable, Figure 1B). The detection window of the bioreporter thus ranged from 0.5 to 45 nM bioavailable Fe.

The effect of other ligands on Fe bioavailability was also assessed in Fraquil where micronutrients (other than Fe) were omitted. In the absence of nutrients, the dose–response curve follows a similar sigmoidal shape as in Figure 1B, which is horizontally displaced to the right. A significant increase of luminescence is observed for bioavailable concentrations of Fe < 10<sup>-7</sup> M and maximal luminescence below 10<sup>-9</sup> M (17).

**Fe Uptake by the Bioreporter.** Intracellular Fe increased linearly over 27 h of exposure. During that period of time, no significant decrease of total dissolved Fe in solution was measured (<11%). Intracellular Fe measured after 12 h in complete Fraquil was used to calculate internalization fluxes (*J*<sub>int</sub>, Figure 2). Iron flux can be predicted by the existence of a simple saturable Fe-transport system (Michaelis–Menten equation, Figure 2; see ref 16 for mathematics and limitations). A maximum uptake capacity of (24 ± 3) amol Fe·cell<sup>-1</sup>·h<sup>-1</sup> occurred when [Fe]<sub>bio</sub> exceeds 4 × 10<sup>-7</sup> M and a half-saturation of transporters is observed at 10<sup>-7</sup> M bioavailable iron. For lower concentrations of bioavailable Fe ([Fe]<sub>bio</sub> ≤ 10<sup>-7</sup> M), *J*<sub>int</sub> is linearly related to [Fe]<sub>bio</sub> in solution (slope close to 1 in a log–log graph (0.92), *r*<sup>2</sup> = 0.97, *n* = 4–8).

Short-term exposure (40 min) limits biological responses such as siderophore induction and secretion, which would confound interpretation. In this case, short-term Fe bioaccumulation can be used to differentiate the cause of the observed enhanced Fe bioavailability, either caused by the excretion of siderophore(s) or by the existence of a high-

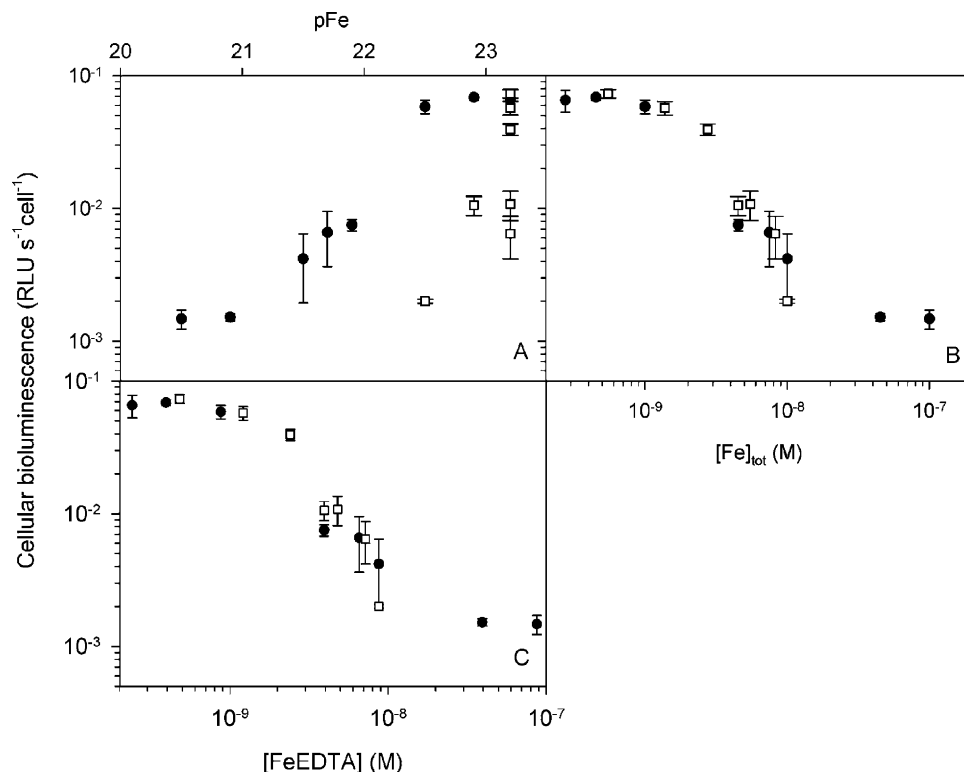


**FIGURE 1.** Cellular bioluminescence measured after 12 h of exposure in Fraquil media with variable iron speciation. The total concentration of Fe was varied ( $4.5 \times 10^{-7}$  to  $2.8 \times 10^{-10}$  M, ●) and [EDTA] was kept constant ( $5 \times 10^{-6}$  M). Both total iron and total EDTA were varied (□). Cellular bioluminescence of the *Synechococcus* iron-bioreporter was plotted against the calculated (MINEQL+) pFe ( $-\log[\text{Fe}^{3+}]$ ) (A),  $[\text{Fe}]_{\text{tot}}$  (B), and  $[\text{FeEDTA}]$ , where  $[\text{FeEDTA}]$  represents 87% of total Fe and is proportional to the concentration of all Fe–EDTA complexes in solution (C). Experiments were performed under light ( $55\text{--}60 \mu\text{mol quanta}\cdot\text{m}^{-2}\cdot\text{s}^{-1}$ ) at  $19^\circ\text{C}$ . Error bars represent the standard deviation ( $n = 4\text{--}8$ ).

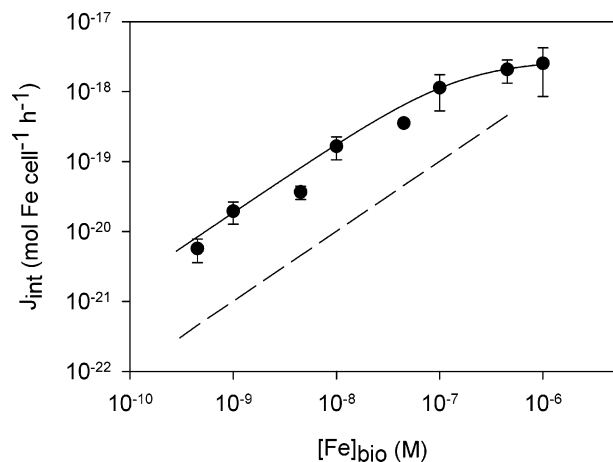


**FIGURE 2.** Internalization uptake fluxes ( $J_{\text{int}}$ ) observed in complete Fraquil media with various iron concentrations.  $J_{\text{int}}$  was related to the  $[\text{Fe}]_{\text{bio}}$  available ( $[\text{Fe}]_{\text{bio}}$ ) in the Fraquil media (i.e.,  $[\text{Fe}]_{\text{tot}}$ ). Experiments were performed under light ( $65\text{--}70 \mu\text{mol quanta}\cdot\text{m}^{-2}\cdot\text{s}^{-1}$ ) at  $19^\circ\text{C}$ . Error bars represent the standard deviation ( $n = 4\text{--}8$ ). The solid line represents the fit to the Michaelis–Menten uptake equation. The dashed line represents the calculated maximal supply of Fe due to spherical diffusion. Diffusive flux was calculated on a per cell basis using the average cellular surface ( $9.2 \pm 1.9 \mu\text{m}^2$ ,  $n = 58$ ).

affinity iron-transport system. Short-term bioaccumulation experiments were performed in the presence of  $10^{-7}$  M  $\text{Fe}_{\text{tot}}$  and various concentrations of DFB, EDTA, and CDTA under light (Figure 3). Increasing [DFB] reduced Fe uptake, whereas increasing the concentration of EDTA and CDTA up to  $10^{-6}$  M failed to reduce Fe uptake with respect to uptake in the absence of ligands. Indeed, small additions of EDTA sig-

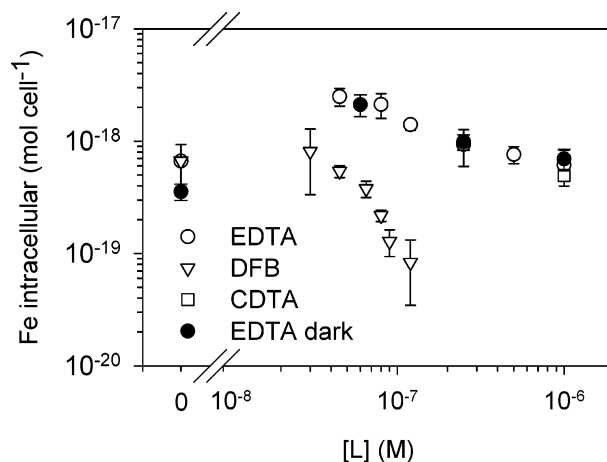


**FIGURE 3.** Intracellular iron following a short-term (40 min) incubation in  $10^{-7}$  M iron in the presence of various concentrations of synthetic ligands. Experiments were performed under light ( $65\text{--}70 \mu\text{mol quanta}\cdot\text{m}^{-2}\cdot\text{s}^{-1}$ , open symbols) and under dark (closed symbols) at  $19^\circ\text{C}$ . Error bars represent the standard deviation ( $n = 4$ ).

nificantly improved Fe biological uptake, probably due to solubilization of Fe by EDTA. The Fe-uptake capacity of the bioreporter was not affected by Fe-replete status since cells grown in medium 1 ( $[\text{Fe}'] = 14 \mu\text{M}$ ) showed similar intracellular content after 40 min of exposure (data not shown). These results suggest that the contribution of Fe bound to EDTA to Fe bioavailability was not due to the presence of siderophore(s) in solution. In the presence of EDTA, no significant differences in Fe uptake were observed when experiments were performed in the dark (Figure 3).

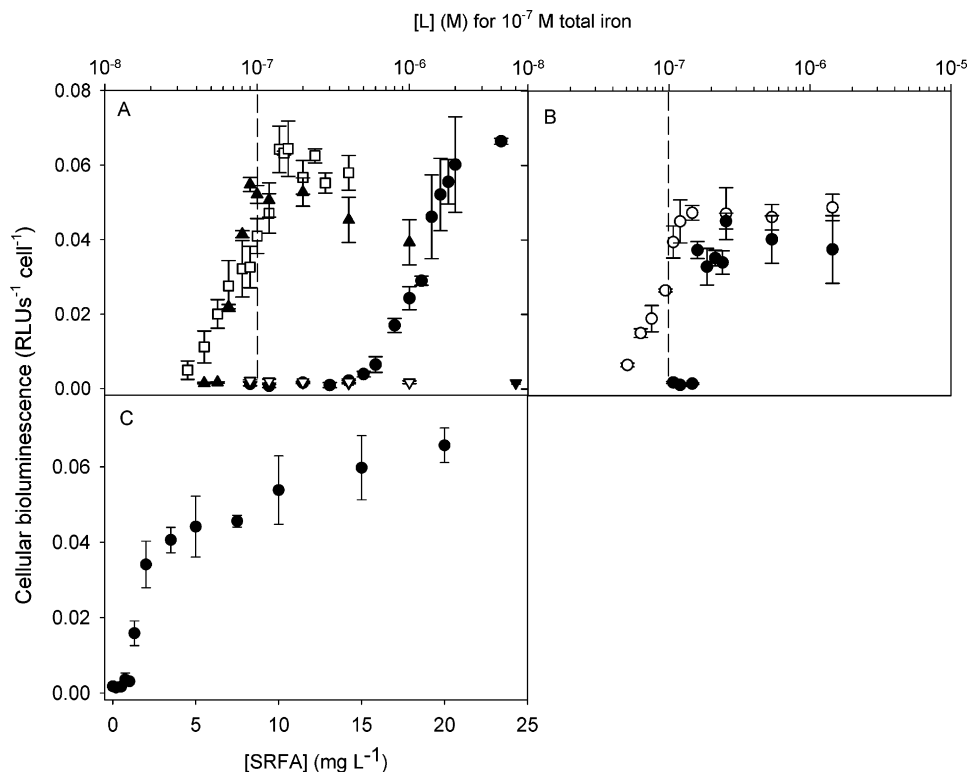


**FIGURE 4.** Effect of a titration of  $10^{-7}$  M  $[\text{Fe}]_{\text{tot}}$  using several ligands on the cellular bioluminescence of the *Synechococcus* iron-bioreporter following a 12 h incubation. Effect of various ligands: (A) synthetic organic ligands (EDTA  $\nabla$ , DTPA  $\square$ , CDTA  $\nabla$ , HEBD  $\blacktriangle$ , and 8HQS  $\bullet$ ) and (B) siderophore-like ligands (DFB  $\circ$ , ferrichrome  $\bullet$ ). (C) The effect of natural organic ligand (SRFA) on cellular bioluminescence was also assessed. Experiments were performed under light ( $65\text{--}70 \mu\text{mol quanta}\cdot\text{m}^{-2}\cdot\text{s}^{-1}$ ) at  $19^\circ\text{C}$ . Error bars represent the standard deviation ( $n = 4\text{--}8$ ).

**Definition of Fe Bioavailability Sensed by *Synechococcus* PCC 7942.** For Fe complexes ( $\text{FeL}$  such as  $\text{FeEDTA}$ ) to become bioavailable, an exchange of ligand either to a siderophore in solution or to a high-affinity protein on the surface of the organism ( $\text{FeX}$ ) must generally occur. The stability constants of the two Fe complexes ( $K_{\text{FeX}}$  and  $K_{\text{FeL}}$ ) and concentrations of ligands (L and X) will determine if the exchange of ligand occurs (see above). In these experiments the nature and concentration of the biological binding sites ( $K_{\text{FeX}}$  and  $[\text{X}]$ ) remained constant, whereas  $K_{\text{FeL}}$  and  $[\text{L}]$  varied. Several types of ligands with various binding groups and binding affinities (Table 2) were used to titrate  $10^{-7}$  M total Fe in Fraquil medium in the absence of other trace metals and organic ligands. At this concentration of  $\text{Fe}_{\text{tot}}$ , no significant cellular luminescence was observed. No increase of bioluminescence was expected if the added ligand does not decrease Fe bioavailability. On the other hand, if the Fe complex formed (assuming a 1:1 Fe complex [see Table 2 for stoichiometry of the complex formed]) and no significant competitive binding by Ca, Mg, and H) was not bioavailable to the bioreporter then the cellular bioluminescence would be expected to increase with  $[\text{L}]$  up to  $[\text{L}] = [\text{Fe}] = 10^{-7}$  M, (since maximal bioluminescence was observed below  $10^{-9}$  M  $\text{Fe}_{\text{bio}}$ ). The ligands DFB, HEBD, ferrichrome, DTPA, and 8HQS effectively decreased Fe bioavailability sensed by the bioreporter (Figures 4A and 4B). In contrast, increasing [EDTA] and [CDTA] up to  $4\text{--}5 \mu\text{M}$  did not increase bioluminescence, as noted above (Figures 1C and 3).

The relative bioavailability (Figure 5) of the organically complexed iron to *Synechococcus* can be determined by considering the ratio of the observed to the predicted concentration of ligand that is required to achieve maximal bioluminescence (assuming a nonbioavailable complex, i.e., relative bioavailability = 1). In this case, strong Fe complexes with log conditional stability constant ( $K^*$ )  $> 28.1$  were not

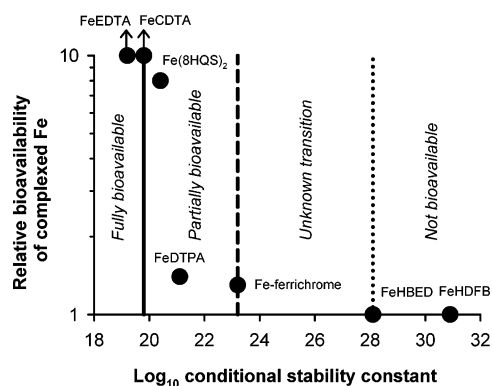


**FIGURE 5.** Relative bioavailability of several Fe complexes to a cyanobacterial Fe-bioreporter as a function of their conditional stability constant. Relative bioavailability is calculated as the ratio of the observed concentration of ligand to the predicted concentration of ligand to achieve the level of maximal response (bioluminescence) of the bioreporter. The observed concentration of ligand is derived from a titration of  $10^{-7}$  M total Fe with the ligand of interest. The predicted concentration of the ligand is determined by thermodynamic considerations as the concentration of ligand that decreases bioavailable Fe to a concentration of  $10^{-9}$  M, the threshold where cellular luminescence becomes maximal under the conditions use in these experiments. At a ratio of unity, the Fe complex is nonbioavailable; fully bioavailable Fe complexes are considered to have a ratio of  $\geq 40$ .

bioavailable (e.g., DFB and HEBD; Table 2). However, relatively weak ligands ( $K^* \leq 19.8$ ) such as EDTA and CDTA were fully bioavailable (i.e., relative bioavailability  $> 50$  and  $40$ , respectively, Figure 5). In accordance with ligand exchange considerations, intermediate Fe complexes ( $K^* 20.4\text{--}23.2$ ) such as ferrichrome, DTPA, and 8HQS were partially bio-

available, with a decrease in Fe-complex bioavailability concomitant with an increase in Fe-binding affinity (i.e., maximal luminescence observed for 1.3-, 1.4-, and 8-fold excess of predicted [L] considering nonbioavailable Fe complexes of ferrichrome, DTPA, and 8HQS, respectively, Figure 5). The bioavailable fraction of Fe sensed by the bioreporter can then be defined as the sum of  $[\text{Fe}^{3+}] + [\text{Fe}(\text{OH})_x] + [\text{FeL}]_i$  for  $K_{\text{FeLi}}^* < 10^{23.2} \text{ M}^{-1}$ . For organic Fe complexes that are partially bioavailable to *Synechococcus* ( $K^* = 19.8\text{--}23.2$ ), the ratio of the ligand to metal is expected to influence bioavailability.

Suwannee River fulvic acid can reduce the bioavailability of  $10^{-7} \text{ M Fe}_{\text{tot}}$ , as sensed by the bioreporter (Figure 4B). At concentrations of SRFA greater than  $1 \text{ mg}\cdot\text{L}^{-1}$ , an increase of luminescence was observed, indicating that Fe bioavailability was reduced. When the concentration of SRFA increased, a first sharp increase of luminescence (up to  $2 \text{ mg SRFA}\cdot\text{L}^{-1}$ ) followed by a slight increase of luminescence up to the maximal level (reached for  $15 \text{ mg SRFA}\cdot\text{L}^{-1}$ ) was observed (Figure 4C), a response consistent with the existence of two distinct Fe-binding groups for SRFA (Table 2).

## Discussion

**Parameters Limiting Fe Uptake.** The maximal uptake flux for iron, calculated according to Michaelis–Menten kinetics (Figure 2), was similar to that observed for the coccolithophorid *Pleurochrysis carterae* (5). Application of Michaelis–Menten kinetics to trace metal uptake relies on several assumptions (16), such as a rate-limiting internalization process (see below). Limitation of uptake due to both diffusion of bioavailable Fe species and kinetic association/dissociation of Fe with the transporter have been reported (5, 6, 25). To verify which phenomena limited Fe uptake by the *Synechococcus* bioreporter, the apparent internalization constant ( $k_{\text{int}}$ ) was calculated by dividing  $J_{\text{int}}$  to total adsorbed Fe (see ref 15). The small apparent  $k_{\text{int}}$  ( $[5.3 \pm 2.1] \times 10^{-6} \text{ s}^{-1}$ ), ca. 130 times smaller than that for *P. carterae* (5), did not suggest any kinetic limitation with the transporter to Fe bioaccumulation. In fact, this small  $k_{\text{int}}$  results in long turnover time, which might not be realistic with conventional membrane transporters. For small microorganisms, maximal diffusive supply of metal ( $J_{\text{diff}}^{\text{max}}$ ,  $\text{mol}\cdot\text{cm}^{-2}\cdot\text{s}^{-1}$  or  $\text{mol}\cdot\text{cell}^{-1}\cdot\text{h}^{-1}$ ) using the average surface area of *Synechococcus*) can be calculated using radial diffusion considerations (eq 1; (26)), where  $D_{\text{Fe}}$  is the coefficient of diffusion of bioavailable Fe species ( $\text{Fe}_{\text{bio}}$  and  $D_{\text{Fe(III)}} = 5.3 \times 10^{-6} \text{ cm}^2\cdot\text{s}^{-1}$  (27) corrected for  $20^\circ\text{C}$ ) and  $R$  is the cellular radius ( $7.7 \times 10^{-5} \text{ cm}$ ):

$$J_{\text{diff}}^{\text{max}} = (D_{\text{Fe}}/R)[\text{Fe}]_{\text{bio}} \quad (1)$$

The diffusive supply of  $\text{Fe}^{3+}$  alone could not support the measured internalization fluxes to the bioreporter ( $J_{\text{diff}}$   $10^{10}$  times  $< J_{\text{int}}$ ; Figure 2). In light of the  $\text{Fe}'$  model (5, 8), diffusion limitation occurs since the diffusive supply of  $\text{Fe}'$  is smaller (10–20-fold; assuming  $D_{\text{Fe(III)}} = D_{\text{Fe}'}$ ) than the measured uptake fluxes. In this case, a strong concentration gradient of  $\text{Fe}'$  between the solution at equilibrium and the cell surface (where  $[\text{Fe}'] = \text{close to zero}$ ) will induce dissociation of the complexed Fe species (26). Thus, the relative contribution of the complex  $\text{FeL}$  ( $J_{\text{kin}}$ , eq 2 (26)) will directly depend on its dissociation constant ( $k_d$ ) and its diffusion coefficient in the reactive layer around the cell (26). Dissociation ( $k_d$ ) and association ( $k_f$ ) constants can be calculated considering the Eigen–Wilkens mechanism and using ( $k_{-w}$  and outer sphere constant  $[K_{\text{OS}}]$ )

$$J_{\text{kin}} = \mu k_d [\text{FeL}] \quad (2)$$

where  $\mu$  is the reactive layer thickness around the cell ( $\mu = \sqrt{D_{\text{Fe}}/(k_f[L])}$ ).

In an extreme situation, all complexed species can contribute to internalization by becoming bioavailable. It follows that the potential diffusive supply calculated considering all chemical species of Fe present in solution is more than 3 orders of magnitude higher than  $J_{\text{int}}$ .

**Understanding the Contribution of FeEDTA to the Bioavailable Pool.** Iron bound to EDTA was found to contribute to cellular uptake of Fe (Figure 3) but not bioluminescence (Figures 1C and 4A) by the bioreporter. Diffusion limitation (leading to induced  $\text{Fe}$ -complex lability) could enhance the dissociation of the major species present (FeEDTA and FeOHEDTA). Iron is a slowly reactive metal (small  $k_{-w}$ ) for which inorganic complexation with hydroxide has been reported to increase  $k_{-w}$  by more than 5 orders of magnitude in seawater (15). The  $k_{-w}$  for  $\text{Fe}^{3+}$  and  $\text{FeOH}^{2+}$  (15) were used to estimate the respective dissociation of FeEDTA and FeOHEDTA according to eq 2 (26). For both  $\text{Fe}$ –EDTA complexes, the kinetic dissociation cannot explain the high internalization fluxes measured as  $J_{\text{kin}} < J_{\text{int}} - J_{\text{diff max}}$  by 12 versus 4 orders of magnitude for FeEDTA and FeOHEDTA, respectively. Note that in the situation described here, FeOHEDTA is the chemical species that is the most susceptible to contribute to Fe bioavailability. Nonetheless, such calculations rely on several parameters that are still poorly defined (e.g., assumption of an identical  $k_{-w}$  and  $D_{\text{Fe}}$  in fresh and seawaters, effect of ellipsoidal versus spherical cells, effect of diffusion limitation on the induction of chemical lability of chelated iron).

In previous studies, FeEDTA was not found to contribute to Fe uptake by marine phytoplankton (mainly diatoms (5, 7, 25)); these authors conducted Fe-uptake experiments in the dark to avoid photodissociation of FeEDTA and the subsequent production of potentially bioavailable Fe. The negligible effect of photodissociation under the conditions here was demonstrated by short-term uptake experiments performed under light and in the dark. The use of a surface reductase to access Fe can also enhance Fe bioavailability (14); however, a negligible reduction of FeEDTA relative to  $[\text{Fe}']$  was reported for eukaryotic phytoplankton (8). Fe bound to EDTA was also accessible to other organisms which acquire Fe through a surface Fe reductase (e.g., green algae (28)).

The main Fe-uptake route, under Fe limitation, reported in the literature for bacteria and cyanobacteria, including *Synechococcus* PCC 7942 (22), involves siderophore excretion and specific recognition of Fe bound to siderophores (13). In the presence of a siderophore, competitive ligand exchange for Fe is enhanced and equilibrium is displaced toward the formation of the  $\text{Fe}$ –siderophore complex (14). Both the high concentrations and the low conditional stability constant of FeOHEDTA and FeEDTA relative to those of a typical hydroxamate siderophore (Table 2) might favor their dissociation. For the  $\text{Fe}$ -bioreporter derived from *Synechococcus* PCC 7942, an enhancement of Fe bioavailability has been observed after 36 h (17). In addition, the bioreporter grown at high Fe concentrations (medium 1,  $[\text{Fe}'] = 14 \mu\text{M}$ ) was able to access Fe bound to EDTA. Siderophore excretion by the  $\text{Fe}$ -bioreporter in medium 1 is not expected since  $20 \mu\text{M}$  Fe rapidly suppresses the production of siderophores by the freshwater cyanobacterium *Anabaena* (i.e., within the time of analysis using the CASAD assay, H. G. Weger, University of Regina, Regina, SK, Canada, personal communication). However, since siderophores were not directly measured in this study, a basal production cannot be excluded.

**Predicting Fe Bioavailability to the Bioreporter Using Simple and Natural Fe Chelators.** Whether bioavailability of Fe bound to EDTA is due to kinetic dissociation in response to diffusion limitation of  $\text{Fe}'$  or excretion of siderophores cannot be distinguished as both mechanisms rely on the ability of the Fe complex to dissociate. In both cases, the complexed Fe must undergo ligand exchange that is de-

pendent on the respective stability constants. Supporting data were reported for a freshwater cyanobacterium for which the ability to consume Fe was similar for two ligands (EDDHA and DFB) that possessed different structures but had similar affinity constants for Fe(III) (11). The partial bioavailability of FeDFB to *Anabaena* was related to the excretion of a siderophore. Moreover, “weak” Fe complexes FeHEDTA ( $K = 22.3$ , (11)) and FeEDTA ( $K = 27.7$ , this study) and FeCDTA ( $K = 32.7$ , this study) are bioavailable, whereas strong Fe chelates (Fe–HBED,  $K = 41.6$ , this study and (11)) are not accessible to these cyanobacteria. In addition, Fe–DFB, and Fe–ferrichrome are not bioavailable to a bacterial iron-bioreporter (*Pseudomonas putida*), whereas addition of 200 nM EDTA to natural seawater did not reduce iron bioavailability (29).

Natural organic ligands, responsible for the majority of Fe chelation in natural waters (30, 31), are described by two Fe (Fe') conditional stability constants ( $K^*$  from 10 to 13 in seawater determined by CLE-ACSV techniques (30–32)). The conditional stability constants for Fe'–organic ligands in seawater are smaller than that for Fe'–DFB ( $K^* 16.5$ , (30)) and similar to heme-based ligands (i.e., Fe'–protoporphyrin,  $K^* = 12$  (30)). Hutchins et al. (9) report a high capacity for cyanobacteria to utilize an Fe–porphyrin complex. In addition, the ability of the bioreporter to access relatively strongly bound Fe ( $\log K^*_{\text{Fe(III)}} < 23.2$  or  $K^*_{\text{Fe}} < 14$ , this study) begs the question concerning the potential bioavailability of Fe that is “weakly” bound to natural organic ligands.

In natural waters, fulvic acids (FA) are an important fraction of dissolved humic substances (33) that can significantly complex Fe(III) by two major binding sites (34). Our study shows the ability of SRFA ( $>1 \text{ mg}\cdot\text{L}^{-1}$  SRFA) to reduce Fe bioavailability through two Fe-binding sites, with a decrease in Fe bioavailability from  $10^{-7}$  to  $10^{-9} \text{ M Fe}_{\text{tot}}$  by  $15 \text{ mg}\cdot\text{L}^{-1}$  SRFA. The complex nature of FA and poorly characterized binding capacity of SRFA for Fe results in many nonquantified parameters that renders modeling of potential ligand exchange difficult. Fulvic acid was reported to decrease the growth of freshwater cyanobacteria (11, 35); for *Microcystis* and an [Fe'] of  $10^{-7.4} \text{ M}$  in a complete growth medium,  $2 \text{ mg}\cdot\text{L}^{-1}$  FA reduced by a factor of ca. 10 the amount of chlorophyll *a* at stationary phase, whereas a complete inhibition of growth was reported for  $10 \text{ mg}\cdot\text{L}^{-1}$  FA. Since most dissolved organic carbon (DOC) in lakes is composed of humic substances, a DOC concentration as low as  $0.5 \text{ mg}\cdot\text{L}^{-1}$  (e.g., Lake Superior) could significantly decrease the bioavailability of the 1–10 nM total dissolved Fe present in the pelagic areas of this lake (36). Since natural waters contain trace metals (e.g., Al, Cu) other than Fe at appreciable concentrations, it is possible that these other metals act to increase Fe bioavailability by competitive interaction with FA in solution. Further investigation of these interactions is possible using the Fe-bioreporter as the analytical tool to assess Fe bioavailability.

In conclusion, this study provides insight into the contribution of chelated iron to bioavailability as sensed by an environmentally relevant phytoplanktonic bioreporter (17). Under slight iron-deficient conditions, iron bioaccumulation is limited by diffusion of Fe' to the cell surface and iron bioavailability can be predicted by considering the conditional stability constant of the chelated iron. Under more severe iron deficiency, secretion of siderophores and/or induction of specific membrane-associated receptor(s) (6, 13, 14) will further enhance iron bioavailability and Fe complexes with conditional stability constants greater than the  $10^{23.2} \text{ M}^{-1}$  could then become bioavailable to this microorganism. In addition, sunlight and UV photodissociation of natural ligands (37), as well as biologically enhanced Fe(III) reduction (38), might be important parameters affecting bioavailability under natural conditions. Although

assessment of iron bioavailability in natural waters remains difficult, the use of this Fe-bioreporter is promising. Further development and simultaneous use of other prokaryotic (29) and eukaryotic Fe-bioreporters will further advance our understanding of Fe bioavailability to phytoplankton.

## Acknowledgments

This research was supported by a collaborative Grant from the National Science Foundation (Chem Oce No. 0327730) to M.R.T. and RML McKay and GS Bullerjahn of Bowling Green State University. C.S.H. received funding from the Swiss National Science Foundation (No. PBGEA-104637) and Clarkson University. We thank Claude Fortin for useful comments on this manuscript and Sonya Havens for routine GFAAS analysis of Fe content in media. This is Contribution No. 275 of the Clarkson University Center for the Environment.

## Literature Cited

- Boyd, P. Ironing out algal issues in the Southern Ocean. *Science* **2004**, *304*, 396–397.
- Twiss, M. R.; Auclair, J.-C.; Charlton, M. N. An investigation into iron-stimulated phytoplankton productivity in epipelagic Lake Erie during thermal stratification using trace metal clean techniques. *Can. J. Fish. Aquat. Sci.* **2000**, *57*, 86–95.
- Sterner, R. W.; Smutka, T. M.; McKay, R. M. L.; Xiaoming, Q.; Brown, E. T.; Sherrell, R. M. Phosphorus and trace metal limitation of algae and bacteria in Lake Superior. *Limnol. Oceanogr.* **2004**, *49*, 495–507.
- Buesseler, K. O.; Andrews, J. E.; Pike, S. M.; Charette, M. A. The effects of iron fertilization on carbon sequestration in the Southern Ocean. *Science* **2004**, *304*, 414–17.
- Hudson, R. J. M.; Morel, F. M. M. Iron transport in marine phytoplankton: kinetics of cellular and medium coordination reactions. *Limnol. Oceanogr.* **1990**, *35*, 1002–20.
- Hudson, R. J. M. Which aqueous species control the rates of trace metal uptake by aquatic biota? Observations and predictions of nonequilibrium effects. *Sci. Total Environ.* **1998**, *219*, 95–115.
- Anderson, M. A.; Morel, F. M. M. The influence of aqueous iron chemistry on the uptake of iron by the coastal diatom *Thalassiosira weissflogii*. *Limnol. Oceanogr.* **1982**, *27*, 789–813.
- Shaked, Y.; Kustka, A. B.; Morel, F. M. M. A general kinetic model for iron acquisition by eukaryotic phytoplankton. *Limnol. Oceanogr.* **2005**, *50*, 872–82.
- Hutchins, D. A.; Witter, A. E.; Butler, A.; Luther, G. W., III. Competition among marine phytoplankton for different chelated iron species. *Nature* **1999**, *400*, 858–61.
- Maldonado, M. T.; Price, N. M. Utilization of iron bound to strong organic ligands by plankton communities in the subarctic Pacific Ocean. *Deep-Sea Res.* **1999**, *46*, 2447–73.
- Gress, C. D.; Treble, R. G.; Matz, C. J.; Weger, H. G. Biological availability of iron to the freshwater cyanobacteria *Anabaena flos-aquae*. *J. Phycol.* **2004**, *40*, 879–86.
- Durham, K. A.; Porta, D.; Twiss, M. R.; McKay, R. M. L.; Bullerjahn, G. S. Construction and initial characterization of a luminescent *Synechococcus* sp. PCC 7942 Fe-dependent bioreporter. *FEMS Microbiol. Lett.* **2002**, *209*, 215–21.
- Wilhelm, S. W. Ecology of iron-limited cyanobacteria: a review of physiological responses and implications for aquatic systems. *Aquat. Microb. Ecol.* **1995**, *9*, 295–303.
- Völker, C.; Wolf-Gladrow, D. A. Physical limits on iron uptake mediated by siderophores or surface reductases. *Mar. Chem.* **1999**, *65*, 227–44.
- Hudson, R. J. M.; Morel, F. M. M. Trace metal transport by marine microorganisms: implications of metal coordination kinetics. *Deep-Sea Res.* **1993**, *40*, 129–50.
- Wilkinson, K. J.; Buffle, J. Critical evaluation of physicochemical parameters and processes for modelling the biological uptake of trace metals in environmental (aquatic) systems. In *Physicochemical Kinetics and Transport at Biointerfaces*; Van Leeuwen, H. P., Köster, W. Eds.; John Wiley & Sons: Chichester, U.K., 2004; pp 445–533.
- Hassler, C. S.; Twiss, M. R.; McKay, R. M. L.; Bullerjahn, G. S. Optimization of iron-dependent cyanobacterial (*Synechococcus*, Cyanophyceae) bioreporters to measure iron bioavailability. *J. Phycol.*, in press.

- (18) Escolar, L.; Pérez-Martín, J.; de Lorenzo, V. Opening the iron box: transcriptional metalloregulation by the Fur protein. *J. Bacteriol.* **1999**, *181*, 6223–29.
- (19) Rippka, R.; Deruelles, J.; Waterbury, J. B.; Herdman, M.; Stanier, R. Y. Genetic assignments, strain histories, and properties of pure cultures of cyanobacteria. *J. Gen. Microbiol.* **1979**, *111*, 1–61.
- (20) Morel, F. M. M.; Westall, J. C.; Rueter, J. G., Jr.; Chaplick, J. P. *Description of algal growth media AQUIL and FRAQUIL*; Technical Note No. 16; R. M. Parsons Laboratory for Water Resources and Hydrodynamics, Massachusetts Institute of Technology: Cambridge, MA, 1975.
- (21) Price, N. M.; Harrison, G. I.; Hering, J. G.; Hudson, R. J.; Nirel, P. M. V.; Palenik, B.; Morel, F. M. M. Preparation and chemistry of the artificial algal culture medium AQUIL. *Biol. Oceanogr.* **1989**, *6*, 443–61.
- (22) Wilhelm, S. W.; Trick, C. G. Iron-limited growth of cyanobacteria: multiple siderophore production is a common response. *Limnol. Oceanogr.* **1994**, *39*, 1979–84.
- (23) Tovar-Sanchez, A.; Sañudo-Wilhelmy, S. A.; Garcia-Vargas, M.; Weaver, R. S.; Popels, L. C.; Hutchins, D. A. A trace metal clean reagent to remove surface-bound iron from marine phytoplankton. *Mar. Chem.* **2003**, *82*, 91–99.
- (24) Hassler, C. S.; Slaveykova, V. I.; Wilkinson, K. J. Discriminating between intra- and extracellular metals using chemical extractions. *Limnol. Oceanogr. Methods* **2004**, *2*, 237–47.
- (25) Sunda, W. G.; Huntsman, S. A. Iron uptake and growth limitation in oceanic and coastal phytoplankton. *Mar. Chem.* **1995**, *50*, 189–206.
- (26) Pinheiro J. P.; van Leeuwen H. P. Metal speciation dynamics and bioavailability. 2. Radial diffusion effects in the microorganism range. *Environ. Sci. Technol.* **2001**, *35*, 890–900.
- (27) Li, Y. H.; Gregory, S. Diffusion of ions in seawater and deep-sea sediments. *Geochim. Cosmochim. Acta* **1974**, *38*, 704–14.
- (28) Collins, C. M.; Anderson, A. M.; Weger, H. G. Iron acquisition by the green alga *Selenastrum minutum*: growth in iron-limited chemostats and effects of chelator stability constant. *Arch. Hydrobiol.* **2001**, *151*, 283–99.
- (29) Mioni, C. E.; Howard, A. M.; DeBruyn, J. M.; Bright, N. G.; Twiss, M. R.; Applegate, B. M.; Wilhelm, S. W. Characterization and field trials of a bioluminescent bacterial reporter of iron bioavailability. *Mar. Chem.* **2003**, *83*, 31–46.
- (30) Rue, E. L.; Bruland, K. W. Complexation of Fe(III) by natural organic ligands in the Central North Pacific as determined by a new competitive ligand equilibration/adsorptive cathodic stripping voltammetric method. *Mar. Chem.* **1995**, *50*, 117–38.
- (31) Powell, R. T.; Wilson-Finelli, A. Importance of organic Fe complexing ligands in the Mississippi River plume. *Estuarine, Coastal Shelf Sci.* **2003**, *58*, 757–63.
- (32) Macrellis, H. M.; Trick, C. G.; Rue, E. L.; Smith, G.; Bruland, K. W. Collection and detection of natural iron-binding ligands from seawater. *Mar. Chem.* **2001**, *76*, 175–87.
- (33) McKnight, D. M.; Hood, E.; Klapper, L. Trace organic moieties of dissolved organic material in natural waters. In *Aquatic Ecosystems: Interactivity of Dissolved Organic Matter*; Findlay, S.E.G., Sinsabaugh, R. L., Eds.; Elsevier: New York, 2003; pp 71–96.
- (34) Tipping, E.; Rey-Castro, C.; Bryan, S. E.; Hamilton-Taylor, J. H. Al(III) and Fe(III) binding by humic substances in freshwaters and implications for trace metal speciation. *Geochim. Cosmochim. Acta* **2002**, *66*, 3211–24.
- (35) Imai, A.; Fukushima, T.; Matsushige, K. Effects of iron limitation and aquatic humic substances on the growth of *Microcystis aeruginosa*. *Can. J. Fish. Aquat. Sci.* **1999**, *56*, 1929–37.
- (36) Field, P. M.; Sherrell, R. M. Direct determination of ultra-trace levels of metals in freshwater using desolvating micronebulization and HR-ICP-MS: application to Lake Superior waters. *J. Anal. At. Spectrom.* **2003**, *18*, 254–9.
- (37) Rijkenberg, M. J. A.; Fischer, A. C.; Kroon, J. J.; Gerringa, L. J. A.; Timmermans, K. R.; Wolterbeek, H. T. The influence of UV irradiation on the photoreduction of iron in the Southern Ocean. *Mar. Chem.* **2005**, *93*, 119–29.
- (38) Shaked, Y.; Erel, Y.; Sukenik, A. Phytoplankton-mediated redox cycle of iron in the epilimnion of Lake Kinneret. *Environ. Sci. Technol.* **2002**, *36*, 460–7.

Received for review September 9, 2005. Revised manuscript received February 3, 2006. Accepted February 6, 2006.

ES051795I